Forest Ecology and Management 556 (2024) 121730

Contents lists available at ScienceDirect

Forest Ecology and Management

journal homepage: www.elsevier.com/locate/foreco

Aridification increases growth resistance of Atlas cedar forests in NW Algeria

Mohamed Sarmoum [a], J. Julio Camarero [b,*], Fatiha Abdoun [c]

[a] *Laboratory of Plant Physiology and Soil Culture, Faculty of Nature and Life Sciences, Ibn Khaldoun University, PO Box 78, Zaaroura, Tiaret, Algeria*
[b] *Instituto Pirenaico de Ecología (IPE-CSIC), Avda.Montañana 1005, 50192 Zaragoza, Spain*
[c] *Laboratory of Plant Ecology and Environment, Faculty of Biological Sciences, University of Science and Technology Houari Boumédiène, BP 32 El Alia, BabEzzouar, Alger, Algeria*

ARTICLE INFO

Keywords:
Cedrus atlantica
Drought
NAO
Radial growth
Resilience index
Resistance index

ABSTRACT

A warmer climate will increase aridity and threaten forest persistence in xeric areas. This is the case of some Atlas cedar (*Cedrus atlantica*) forests showing recent growth decline, dieback and high mortality rates in North Africa. A lower resistance to drought, manifested as stronger growth loss, could increase the drought-related mortality risk in these forests as has been found for gymnosperms worldwide. It could be also expected that changes in dryness are linked to large-scale atmospheric circulation patterns such as the North Atlantic Oscillation (NAO). We tested these hypotheses by analyzing growth resilience indices (resilience, recovery, resistance) derived from tree-ring data. We sampled nine Atlas cedar plots located in north-western Algeria, where climate shifted towards drier conditions in the 1980s. In these forests, drier winters, associated to positive NAO phases, constrained tree growth and resistance, two outputs of the drought impact. During dry years, the resilience index decreased as elevation increased. The association between cedar growth resistance and drought severity is strengthening: the drier the climate conditions, the lower the growth resistance. Resistance also showed a significant higher temporal variability in 8 out of 9 plots as drought intensified. These findings have allowed identifying the increase in the temporal variability of growth resistance as a new early-warning signal of drought stress.

1. Introduction

Climate warming is spatially heterogeneous with some regions showing greater increases in temperature and aridity and stronger intensification of the hydrological cycle than others (Padrón et al., 2020). For instance, record droughts are projected for the Mediterranean Basin in the mid-21st century under high-emission scenarios (Satoh et al., 2022). These projections are worrisome for northern Africa forest ecosystems, which have already been negatively affected by historically unprecedented droughts since the 1980s (Touchan et al., 2011). Indeed, several Mediterranean mountain forests have shown recent dieback and mortality episodes in response to those record dry spells and increasing aridification (Allen et al., 2015; Camarero et al., 2015; Heydari et al., 2023).

Atlas cedar (*Cedrus atlantica* [Endl.] Manetti ex Carrière) mountain forests have been negatively impacted by recent droughts showing high mortality rates in some areas of Morocco and Algeria, where they have been replaced by more drought-tolerant tree species (Bentouati, 2008; Sarmoum et al., 2018, 2019; Messaoudene et al., 2013). In addition, other researchers have found a long-term decline in radial growth in these cedar forests, an increasing growth synchrony among trees and a high responsiveness to precipitation (Kherchouche et al., 2012, 2013; Linares et al., 2011, 2013; Slimani et al., 2014). However, in a recent review it was found a gradual increase in inter-annual growth variability and a decrease in growth synchrony ca. 20 years before mortality of several conifer species (Cailleret et al., 2019). Nevertheless, that study did not include Atlas cedar which limits our understanding on post-drought growth resilience, i.e. the capacity to return to baseline growth levels, in these threatened tree populations.

Severe water shortage reduces forest growth and productivity, but can also impair the capacity of growth recovery or resilience after drought leading to legacy effects (Anderegg et al., 2015; Gazol et al., 2017; Camarero et al., 2018). In conifers, low post-drought growth resilience makes trees prone to die (DeSoto et al., 2020). Therefore, declining Algerian Atlas cedar forests provide a suitable setting to study the relationships between climate, drought and growth resilience.

* Corresponding author.
E-mail addresses: jjcamarero@ipe.csic.es (J.J. Camarero), fatabdoun@yahoo.fr (F. Abdoun).

https://doi.org/10.1016/j.foreco.2024.121730
Received 21 November 2023; Received in revised form 22 January 2024; Accepted 23 January 2024
Available online 1 February 2024

However, forecasting the future of these forests require early warning signals for anticipating abrupt or imminent transitions between alternative states, for instance from healthy to declining or dying conditions (Scheffer et al., 2009; Dakos et al., 2008, 2015). Growth resilience indices could be used to develop early warning signals of impending forest dieback. Further, determining the resilience of trees to drought is an essential key for forest management and new planting or ecological restoration programs in the face of aridification trends (Wang et al., 2023). For instance, managing Atlas cedar stands to make them more structurally diverse could reduce their vulnerability to drought (Navarro-Cerrillo et al., 2013).

In a previous study on western Algerian Atlas cedar forests, we found growth decline in most stands since the 1980–1990s when climate rapidly warmed and dried leading to dieback and high mortality rates in some sites, particularly on marl and sandstone substrates and at low elevation (Navarro-Cerrillo et al., 2019; Sarmoum et al., 2019). This work aims to fill the research gap related to the past changes in growth resilience of these forests and how they were driven by regional climate variability, explicitly considering large-scale atmospheric circulation patterns, and drought severity. Furthermore, it is still understudied if Atlas cedar growth resilience depends on circulation patterns such as those captured by the North Atlantic Oscillation (NAO), index which impact winter climate conditions and tree growth in the western Mediterranean Basin (Hurrell, 1995; Camarero, 2011). The NAO variability is related to shifts in the position of the Iceland low-pressure and the Azores high-pressure systems linked to changes in the direction and strength of westerly winds in southern Europe (Hurrell et al., 2003). High (low) NAO values in winter are linked to low (high) precipitation over the western Mediterranean Basin (Hurrell and Van Loon, 1997).

Our specific aims are: (i) to analyze the changes in growth resilience of Atlas cedar in north-western Algeria, and (ii) to quantify how NAO, climate variability and drought severity drive Atlas cedar growth resilience. We expect that wet-cool conditions, related to low NAO values in winter, enhance growth and its resilience components, particularly resistance, an output of the drought impact on growth, as compared with previous years, and also resilience, a measure of the capacity to recover pre-drought growth levels after a drought (cf. Lloret et al., 2011).

2. Material and methods

2.1. Study area

This study was carried out in the Ouarsenis massif located in north-western Algeria. Two Atlas cedar sites and nine plots (Ain Antar –two plots– and Theniet El Had –seven plots) were sampled (Table 1, Fig. S1). This massif is subjected to Mediterranean climate conditions with cold and wet winters and dry and hot summers. The mean monthly maximum and minimum temperatures are 21.5 ± 0.6 ºC and 10.2 ± 0.5 ºC, respectively. The warmest and coldest months are July (with a mean maximum temperature of 34.2 ºC) and January (with a mean minimum temperature of 2.6 ºC), respectively. The average annual rainfall (± SD) recorded in the study area during the period 1950–2020 is 500 ± 101 mm with a wide year-to-year variability (e.g., a maximum of 733 mm was recorded in 1973, whereas a minimum of 308 mm was recorded in 2000). In fact, the coefficient of variation of precipitation is 20.3%, whilst those of mean maximum and minimum temperatures are 2.6% and 5.3%, respectively.

The dry period, when monthly precipitation is lower than two times the mean monthly temperature (Gaussen, 1956), lasts from June to September. According to this criterion, July and August are the driest months, whereas January and February are the wettest months. The lowest and highest monthly precipitations are recorded in July (6 mm) and February (82 mm), respectively.

2.2. Material

The Ain Antar forest covers an area of ca. 500 ha. Atlas cedar appears from an elevation of 1000 m mixed with Aleppo pine, and dominates at high elevations (> 1500 m). Soils are developed on limestone bedrocks leading to rocky, shallow soils. The bioclimate is sub-humid to humid (Sarmoum et al., 2018). This pure cedar forest is not strictly protected, but it is only used for grazing and sporadic timber harvesting. The Theniet El Had forest is a protected area managed as National Park since 1983. It covers an area of approximately 1000 ha. The cedar occupies elevations ranging from 1300 to 1786 m a.s.l. and experiences sub-humid and humid bioclimates. Soils are basic and developed on carbonaceous sandstone bedrocks leading to deep soils. Cedar stands are pure or mixed with oak species such as *Quercus ilex* and *Quercus faginea* (Sarmoum et al., 2018, 2019). The diameter at 1.3 m (dbh, diameter at breast height) and height of dominant Atlas cedar trees range 37.5 – 60.0 cm and 11 – 14 m, respectively, with most dominant trees (66%) having ages between 100 and 160 years (Sarmoum et al., 2018).

The Atlas cedar tolerates well short droughts, but it does not display positive values of net photosynthesis at low water potentials, whereas other Mediterranean species such as *Q. ilex* show net carbon uptake under such dry conditions, probably by accessing and using deep water sources (Aussenac and Finkelstein, 1983). The Atlas cedar shows an early stomatal closure and a xylem more vulnerable to embolism than other Mediterranean cedar species from drier regions (Ladjal et al., 2005, 2007). It is a shade-intolerant, long-living species with old individuals reaching ages over 1000 years (Esper et al., 2007). It shows high to moderate growth rates, but young individuals form shallow root systems which cannot uptake deep water sources (Linares et al., 2013).

2.3. Field sampling and tree-ring methods

The sampling of cores was carried out in nine rectangular plots (50 m x 20 m), which were placed in representative areas of each stand. The diameter of cored cedar trees was measured at 1.3 m and we also recorded: elevation, exposure, forest composition and bedrock type. In each plot, between 10 and 15 dominant and co-dominant trees were cored at 1.3 m using a Pressler increment borer. Two cores were extracted from each tree perpendicular to the stem and to the maximum slope in opposite directions.

The cores were air dried, mounted on wooden supports, sanded and visually cross-dated under the binocular using dendrochronological

Table 1
Main features of the Atlas cedar study plots.

Site	Plot	Latitude N	Longitude E	Elevation (m a.s.l.)	Aspect	Slope (%)	Bedrock type
Ain Antar	AIN1	35° 53′ 34′'	1° 39′ 25′'	1150	NW	20-30	Limestone
	AIN2	35° 53′ 30′'	1° 38′ 48′'	1450	N-NW	50-60	Limestone
Theniet El Had	TOUR1	35° 51′ 44′'	1° 59° 18′'	1550	NE	50-60	Sandstone
	TOUR2	35° 51′ 08′'	1° 57′ 08′'	1700	N	50-60	Sandstone
	OUAR	35° 51′ 50′'	1° 57′ 27′'	1530	SW	50-60	Sandstone
	PEP	35° 53′ 23′'	2° 00′ 02′'	1460	N-NE	20-30	Sandstone
	ROND	35° 52′ 35′'	1° 56′ 00′'	1425	NW	20-30	Sandstone
	DJOUA	35° 52′ 24′'	1° 58′ 25′'	1420	N-NW	30-40	Sandstone
	GUAR	35° 52′ 06′	1° 58′ 01′'	1325	NE	10-20	Sandstone

methods (Stokes and Smiley, 1968; Speer, 2010). Then, tree-ring widths were measured using a LINTAB-TSAP measuring device (TSAP, Heidelberg, Germany) with an accuracy of 0.01 mm. The visual cross-dating was verified by using the COFECHA software (Holmes, 1983), which calculates moving correlations between the individual series and the mean site series of ring-width indices.

The tree-ring width data were normalized and detrended using the dplR program (Bunn, 2008, 2010; Bunn et al., 2023) in the R statistical software (R Core Team, 2023). Spline (30-year long) polynomials were fitted to tree-ring width data and then ring-width indices were obtained by dividing observed by fitted values (Fritts, 1976). The resulting individual series of ring-width indices were averaged for each plot using bi-weight robust means. To characterize these standardized chronologies, several statistics were calculated (Fritts, 1976; Briffa and Jones, 1990) on raw ring-width series (mean; SD, standard deviation; AR1, first-order autocorrelation) or on indexed series (MS, mean sensitivity; EPS, Expressed Population Signal; Wigley et al., 1984). A chronology was considered to be well replicated for the period with EPS > 0.85.

The relationships among the nine plot series of ring-width indices were analyzed using Principal Component Analysis (PCA) calculated on the matrix of mean tree-ring width indices per plot with calendar years (January to December) as variables. The PCA was calculated using the vegan R package (Oksanen et al., 2023).

2.4. Climate and SPEI data

Due to the lack of long-term, homogeneous local climate databases we obtained monthly maximum and minimum temperature and summed precipitation data (period 1950–2020) from the 0.5º gridded CRU TS v. 4.07 (Harris et al., 2020). The precipitation falling during the hydrological year was calculated by summing monthly precipitation data from the prior October up to the current September. This precipitation shows a strong positive relationship with tree growth in many dry sites of the western Mediterranean Basin where previous winter precipitation plays a major role as driver of spring growth (Camarero, 2011; Camarero et al., 2022). We also obtained sea surface temperatures (SST) over the western Mediterranean Basin to explore the relationships between cedar growth indices, climate, SSTs and NAO indices. The SST data were obtained at 0.25º resolution from NOAA database (Reynolds et al., 2007). The NAO indices were obtained from the CRU webpage (https://crudata.uea.ac.uk/cru/data//nao/; Jones et al., 1997).

For evaluating drought severity, we used the Standardized Precipitation and Evaporation Index (SPEI, Vicente-Serrano et al., 2010). The SPEI is based on precipitation and temperature data, and it has the advantage of being multiscalar by considering different temporal resolutions of cumulative water balance. Here, we considered 1 to 48-month long SPEI scales. Gridded (0.5º resolution) SPEI values for the period 1950–2020 were obtained for each site from the global SPEI database available at https://spei.csic.es/database.html. To have a longer temporal perspective on drought severity, we also used reconstructed data of the summer Palmer Drought Severity Index (PDSI) from 1800 to 2012. These data corresponded to the 0.5º grid encompassing the study sites and were obtained from the Old World Drought Atlas (Cook et al., 2015).

2.5. Growth resilience indices

The calculation of the resilience indices proposed by Lloret et al. (2011) was carried out for each site chronology and focusing on dry years (SPEI < -1.25). We acknowledge the shortcoming of these indices which do not considering the timing of drought in relation to individual tree growth phenology and climatic conditions in the pre- and post-drought periods (cf. Schwarz et al., 2020). However, their simple and efficient quantification of growth responses to disturbances such as drought make them appropriate for this study. We calculated three resilience indices, namely: (i) Rt, resistance or the difference between the growth index in the drought year (G_d) and that in the preceding n years (G_{Pr}):

$$Rt = G_d / G_{Pr} \quad (1)$$

(ii) Rc, recovery which measures the capacity of trees to recover growth (G_{Po}) after drought.

$$Rc = G_{Po} / G_d \quad (2)$$

(iii) Rs, resilience which quantifies the capacity to recover pre-drought growth levels.

$$Rs = G_{Po} / G_{Pr} \quad (3)$$

We considered intervals of $n = 3$ years for calculating these indices, because this interval encompasses most post-drought legacies (Anderegg et al., 2015). We also noted that there is a negative relationship between Rt and Rc according to their mathematical formulations (Gazol et al., 2018, 2020). These calculations were done year by year to obtain series of the three resilience indices (Camarero et al., 2022). Analyses based on intervals of $n = 2$–4 years yielded similar conclusions (*results not presented*). The calculations of resilience indices were carried out by using the pointRes 2.0 R package (van der Maaten Theunissen et al., 2015, 2021). Resilience values of the selected drought years and of all investigated years were compared among sites using Mann-Whitney tests. Trends in resilience indices were assessed using the Kendall τ statistic. Lastly, changes in the temporal variability were quantified by calculating the coefficient of variation (CV) of the three resilience indices along 20-year intervals shifted year by year. Trends of CV were assessed using the Kendall τ statistic.

2.6. Climate-growth, NAO–growth and SPEI–growth relationships

The climate-growth relationships were assessed by calculating Pearson correlations between climate variables (mean maximum and minimum temperatures, precipitation) or NAO indices and series of ring-width indices considering the common period 1950–2006. Correlations were calculated from prior October to current September and the 0.05 and 0.01 significance levels were considered (Camarero et al., 2022). The Pearson correlations were calculated also between the monthly SPEI values, quantified at time scales from 1 to 48 months, and the sites chronologies of ring-width series. These calculations were done by using the TreeClim R package (Zang and Biondi, 2015). To assess the heterogeneity of relationships between the NAO or SPEI vs. resilience indices, moving correlations were calculated along 20-year intervals with correlations shifted every year. Finally, we also calculated spatial correlations between cedar growth indices, climate variables and SST using the Climate Explorer webpage (https://climexp.knmi.nl/).

3. Results

3.1. Growth variability

The diameters of sampled trees ranged between 23 and 54 cm. Year-to-year growth variability was high with ring-width and mean sensitivity values ranging from 0.93 to 1.42 mm and from 0.23 to 0.40, respectively (Table 2). The first-order autocorrelation varied from 0.61 to 0.83 and increased as tree diameter did ($r = 0.70$, $p = 0.03$). EPS values were higher than 0.85 in all sites. The lowest mean sensitivity and EPS values were found in sites AIN1 and AIN2, which are located on limestone bedrock. The EPS increased as site elevation did ($r = 0.78$, $p = 0.01$). Both MS and EPS were lower in sites on limestone bedrock (e.g., AIN1) than in sites on carbonaceous sandstone (e.g., TOUR1) bedrock (Mann-Whitney $U = -1.93$, $p = 0.05$).

The PCA biplot identified dry years (SPEI < -1.25) with very low growth indices (1983, 1993, 1994, 2000, and 2002) and wet years with high growth (1952, 1972, 1998, and 2006) (Fig. 1a). The PC1 scores were positively correlated with the precipitation of the hydrological

Table 2
Tree size (dbh, diameter at breast height) and tree-ring width statistics. The statistics were calculated for the common period 1950–2006. Variables' abbreviations: AR1, first-order autocorrelation of tree-ring width; MS, mean sensitivity (MS) of standard ring-width indices; EPS, Expressed Population Signal. Values are means ± SD.

Site	dbh (cm)	No. Trees (No. cores)	Timespan	Tree-ring width (mm)	AR1	MS	EPS
AIN1	31.5 ± 2.7	14 (16)	1789–2010	1.08 ± 0.70	0.74	0.23	0.86
AIN2	27.0 ± 2.0	10 (14)	1866–2008	1.14 ± 0.72	0.73	0.25	0.90
TOUR1	54.0 ± 5.5	15 (24)	1850–2009	0.94 ± 0.65	0.80	0.36	0.97
TOUR2	44.0 ± 4.0	10 (14)	1876–2008	1.08 ± 0.78	0.83	0.35	0.96
OUAR	22.8 ± 1.8	12 (23)	1891–2006	0.93 ± 0.41	0.64	0.34	0.98
PEP	45.8 ± 3.5	15 (29)	1857–2009	1.24 ± 0.78	0.75	0.40	0.93
ROND	36.4 ± 3.1	15 (28)	1860–2011	1.20 ± 0.89	0.76	0.29	0.94
DJOUA	41.2 ± 3.6	15 (25)	1870–2006	1.01 ± 0.65	0.78	0.27	0.92
GUAR	32.8 ± 2.0	15 (28)	1910–2006	1.42 ± 0.82	0.61	0.31	0.94

year ($r = 0.73$, $p < 0.001$), whereas the PC2 scores were positively correlated with the mean maximum temperatures of the previous December ($r = 0.73$, $p = 0.005$). All years with very negative growth indices were detected after 1980 in the regional mean series as climate became more arid (Fig. 1b). In a longer temporal context, the drought was more intense in the 2000s (Fig. S2).

3.2. Climate-growth and NAO-growth relationships

Most sites showed positive correlations of growth indices with precipitation of the previous October, current January, February, March, April, May, and September (Fig. 2a). February and spring precipitation were the main drivers of growth and showed spatial correlations over NW Algeria, as the 12-month SPEI, related to SSTs over the western Mediterranean Basin (Fig. S3). Maximum and minimum temperatures showed negative relationships with growth indices from prior October to November, from April to July and in September of the current year, whereas they were positive in December and January (Fig. 2a). Similar relationships were found between climate variables and the regional series of growth indices and also negative associations with January and March NAO indices (Fig. 2b and S4). The cedar growth was highly and positively related to the precipitation of the hydrological year ($r = 0.73$, $p < 0.001$; Fig. 2c).

3.3. Temporal variability of resilience indices

Resilience indices were similar among sites either considering the whole study period (1950–2006) or the dry years (1983, 1993, 1994, 2000, and 2002). Sites AIN1 and AIN2 presented the highest resistance values during dry years (Table 3). Resilience indices remained stable through time (Fig. 3). Neither site nor regional resilience, recovery, and resistance indices showed significant trends (Table 4). In contrast, the temporal variability (CV trend) of the recovery and resistance indices has significantly increased in most sites, particularly after 1980 when drought severity increased (Table 4, Fig. 4). For instance, the CV of resistance showed significant increases in 8 out of 9 sites. However, the CV of resilience has significantly increased in 5 out of 9 sites, and the resilience variability of two sites (AIN2, TOUR2) strongly impacted on the mean series of resilience CV of the 9 plots.

During dry years, the resilience index decreased as elevation increased ($r = -0.691$, $p = 0.039$; Fig. S5). The regional mean series of resilience and resistance indices ($r = 0.59$, $p < 0.001$) and resilience and recovery indices were positively related ($r = 0.47$, $p = 0.0004$), whereas those of resistance and recovery indices were negatively associated ($r = -0.40$, $p = 0.003$).

3.4. Climate-resilience and NAO-resilience relationships

Resilience and resistance indices were positively related to winter-spring (January to April), June and September precipitation, and also with precipitation of the hydrological year in several sites (Fig. 5). In contrast, correlations with temperatures were negative in spring and September, excepting with previous autumn-winter months. The recovery index showed less significant correlations with climate variables than the other two indices. In contrast, the recovery index was positively correlated with the January NAO index in several sites, but negatively in the case of the resistance index (Fig. S6). Similar correlations were found with the mean NAO index from January to March.

3.5. Drought-growth and drought-resilience relationships

The regional series of cedar growth indices showed strong positive correlations with the SPEI, peaking from May to September and for 6- to 16-month long scales (Fig. 6a). Lower correlations were found for the regional resilience index (Fig. 6b), but they were higher in the case of the resistance index peaking from May to August for 6- to 8-month long scales (Fig. 6c). The correlation between the resistance index and the 8-month August SPEI sharply increased since the 1980s onwards (Fig. 7). This resistance-SPEI correlation showed a clear spatial signature across NW Algeria, which was stronger than with February precipitation (Fig. S7). Moreover, resistance and NAO indices from January to March were negatively related since the 1980s, whereas this was not the case for the recovery index (Fig. S8).

4. Discussion

As expected, wet-cool conditions enhanced Atlas cedar growth in the study NW Algerian forests. More importantly, we found a strengthening of the correlation between tree growth resistance and dryness which could be the result of acclimation of surviving trees to warmer and more arid conditions.

It is remarkable that the precipitation of the hydrological year accounted for 53% of the variability in the regional series of cedar ring-width indices. High precipitation levels in January and February were very important for Atlas cedar growth (Fig. 2). Such wet conditions were linked to low NAO indices in those months and warm sea temperatures in spring near the Gibraltar strait. These findings confirm that cedar growth in NW Algeria is very constrained by dry winter conditions prior to tree-ring formation connected to positive NAO phases, as has been observed before in other Atlas cedar forests in the western Mediterranean Basin (Linares et al., 2013; Navarro-Cerrillo et al., 2019; Camarero et al., 2022).

However, most of the aforementioned studies did not explicitly consider growth resilience components as we did here. We found that drought stress not only constrained growth but also resilience (capacity to recover) and, as expected, particularly resistance (measure of the drought impact) which again depended on January-February precipitation. Resistance was negatively related to the January NAO index indicating a northward shift of the storm track leading to below-average precipitation levels across the western Mediterranean Basin (Hurrell and Van Loon, 1997; Camarero, 2011). Such dry winter conditions, associated to positive NAO phases lead to relatively long droughts (6–16 months), usually encompassing the hydrological years, which reduce Atlas cedar growth and resistance making these forests prone to growth decline if arid conditions persist.

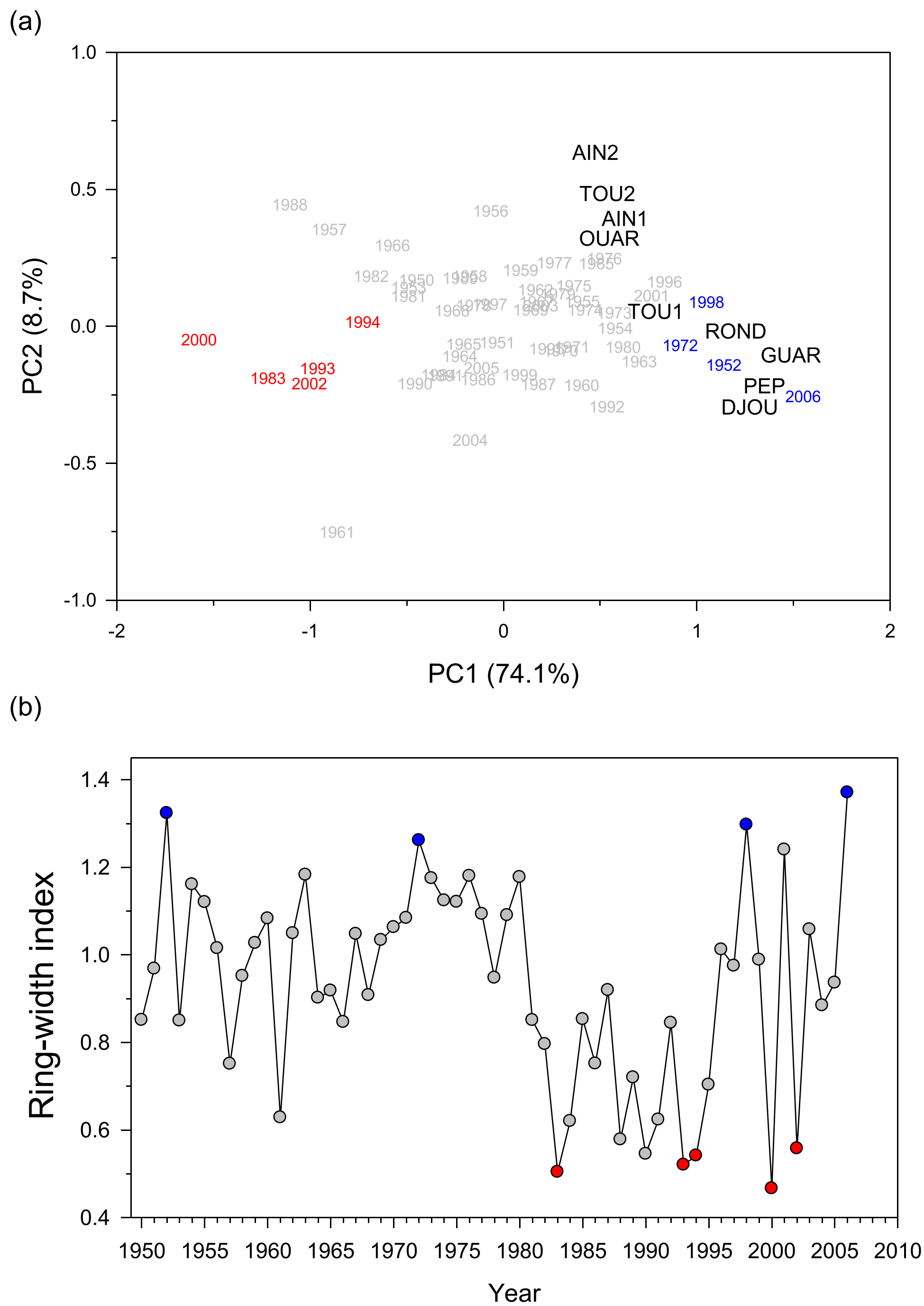

Fig. 1. (a) Biplot showing the sites and pointer years' (very wide –blue characters– or narrow rings –red characters) scores corresponding to the first (PC1) and second (PC2) principal components of a PCA. (b) Regional mean series of ring-width indices showing years of low (red symbols) and high growth (blue symbols).

Moreover, the association between cedar growth resistance and the SPEI is strengthening. This pattern is potentially linked to the multi-decadal NAO variability and could be considered an early-warning signal (cf. Dakos et al., 2008, 2015) and a consequence of forecasted aridification over NW Africa (Giorgi and Lionello, 2008). In the context of the past 500 years, the droughts from the 1980s until the 2000s can be considered very extreme (Esper et al., 2007; Touchan et al., 2011; Cook et al., 2015), but climate models project even warmer and drier winter conditions in NW Africa during the late 21st century (Barcikowska et al., 2018). The higher dependence of growth resistance on drought severity could be anticipating an abrupt shift towards a stronger limitation of tree growth by water shortage passing from cooler and wetter conditions in the 1970s to warmer and drier conditions in the 1980s. Atlas cedar trees could acclimate or die off to warmer and drier conditions (Allen et al., 2015), but our results indicate their capacity to tolerate further droughts will be increasingly dependent on the severity of previous droughts.

Our findings do not evidence a decline in growth resilience of the study forests, despite recent droughts. This contrasts with the increase in the first-order autocorrelation of tree-ring width which preceded the growth decline observed in some of the study stands (Navarro-Cerrillo et al., 2019). In NE Algerian cedar forests showing dieback and high mortality, there was a sharp increase in year-to-year growth variability and also in synchrony in the 1970s as climate progressively warmed and dried (Slimani et al., 2014). Therefore, resilience indices may be more useful to assess post-drought recovery capacity or drought impact rather

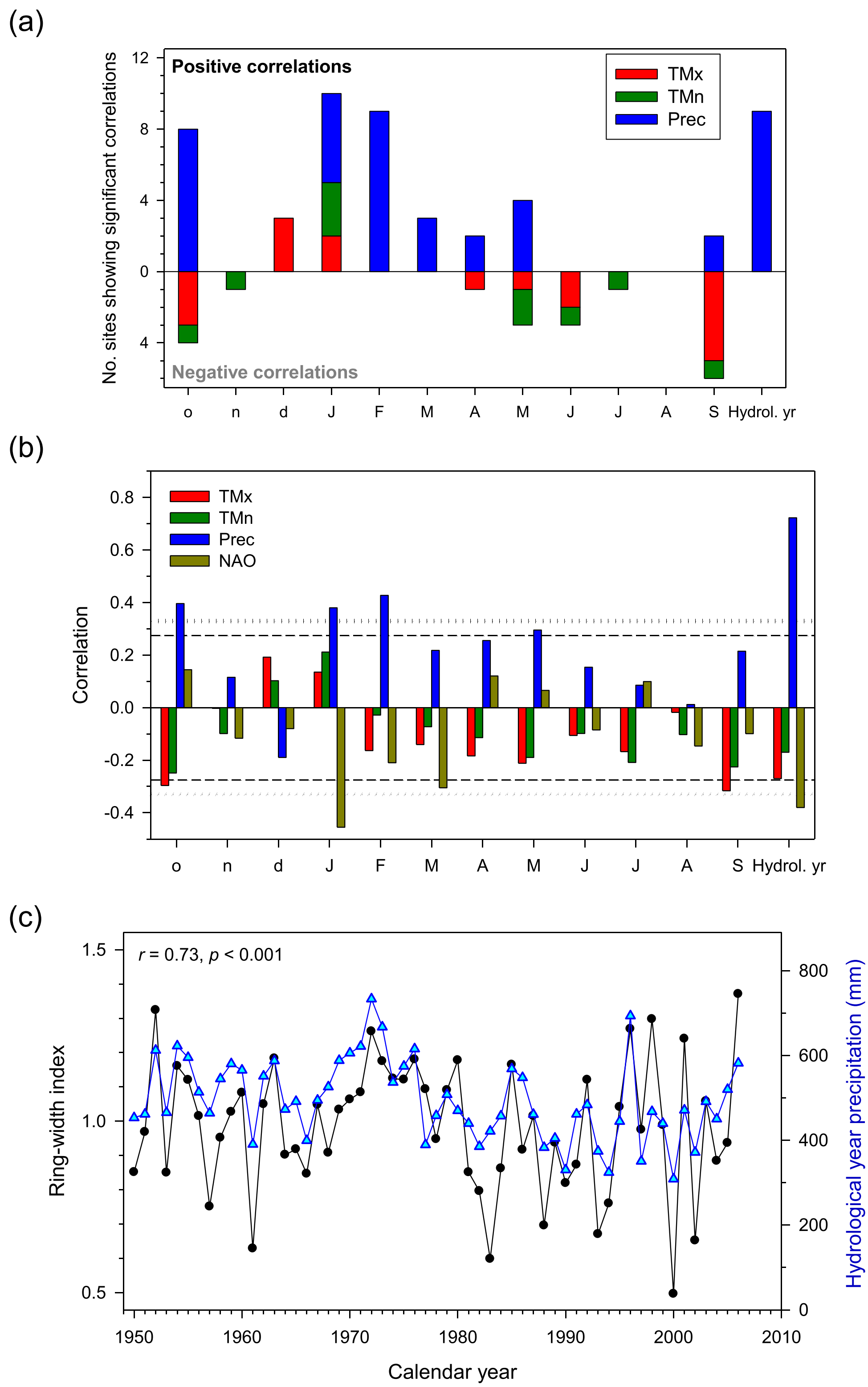

Fig. 2. (a) Number of sites showing significant ($p < 0.05$) positive and negative correlations of site ring-width series with monthly climate variables (TMx, mean maximum temperature; TMn, mean minimum temperature; Prec, total precipitation). (b) Correlations between the regional ring-width series with monthly climate variables and NAO indices and with the precipitation of the hydrological year. Months abbreviated by lowercase and uppercase letters correspond to the previous and current years, respectively. (c) Series of the regional ring-width indices (black dots) and precipitation (blue triangles) of the hydrological year (r, Pearson correlation coefficient; p, probability level).

Table 3
Values of the resilience, recovery, and resistance indices calculated for the period 1950–2006 or considering only recent dry years (1983, 1993, 1994, 2000 and 2002). Resilience indices were calculated using the sites' standardized series of ring-width indices or the regional mean series (last line). Values are means ± SD. Different letters indicate significant ($p < 0.05$) differences among sites according to Mann-Whitney tests.

Site	Period 1950-2006			Dry years		
	Resilience	Recovery	Resistance	Resilience	Recovery	Resistance
AIN1	1.04 ± 0.41	1.03 ± 0.28	1.01 ± 0.26	1.12 ± 0.49	1.40 ± 0.36a	0.77 ± 0.14b
AIN2	0.99 ± 0.28	1.01 ± 0.26	1.00 ± 0.22	0.86 ± 0.27	1.26 ± 0.21a	0.76 ± 0.12b
TOUR1	1.06 ± 0.34	1.06 ± 0.30	1.03 ± 0.29	0.99 ± 0.39	1.44 ± 0.22a	0.71 ± 0.22ab
TOUR2	0.99 ± 0.28	1.01 ± 0.28	1.00 ± 0.24	0.86 ± 0.34	1.48 ± 0.48a	0.58 ± 0.08a
OUAR	1.01 ± 0.20	1.02 ± 0.21	1.00 ± 0.19	0.88 ± 0.11	1.19 ± 0.22a	0.72 ± 0.10ab
PEP	1.07 ± 0.45	1.13 ± 0.48	1.04 ± 0.41	0.88 ± 0.30	1.88 ± 0.26ab	0.46 ± 0.13a
ROND	1.05 ± 0.41	1.07 ± 0.36	1.02 ± 0.33	1.02 ± 0.40	1.60 ± 0.27ab	0.64 ± 0.23ab
DJOUA	1.05 ± 0.42	1.10 ± 0.43	1.03 ± 0.39	0.87 ± 0.22	1.83 ± 0.28ab	0.50 ± 0.16a
GUAR	1.07 ± 0.46	1.12 ± 0.48	1.02 ± 0.38	0.96 ± 0.41	2.08 ± 0.47b	0.45 ± 0.16a
Mean	1.02 ± 0.30	1.03 ± 0.27	1.01 ± 0.25	0.93 ± 0.30	1.50 ± 0.20ab	0.61 ± 0.12a

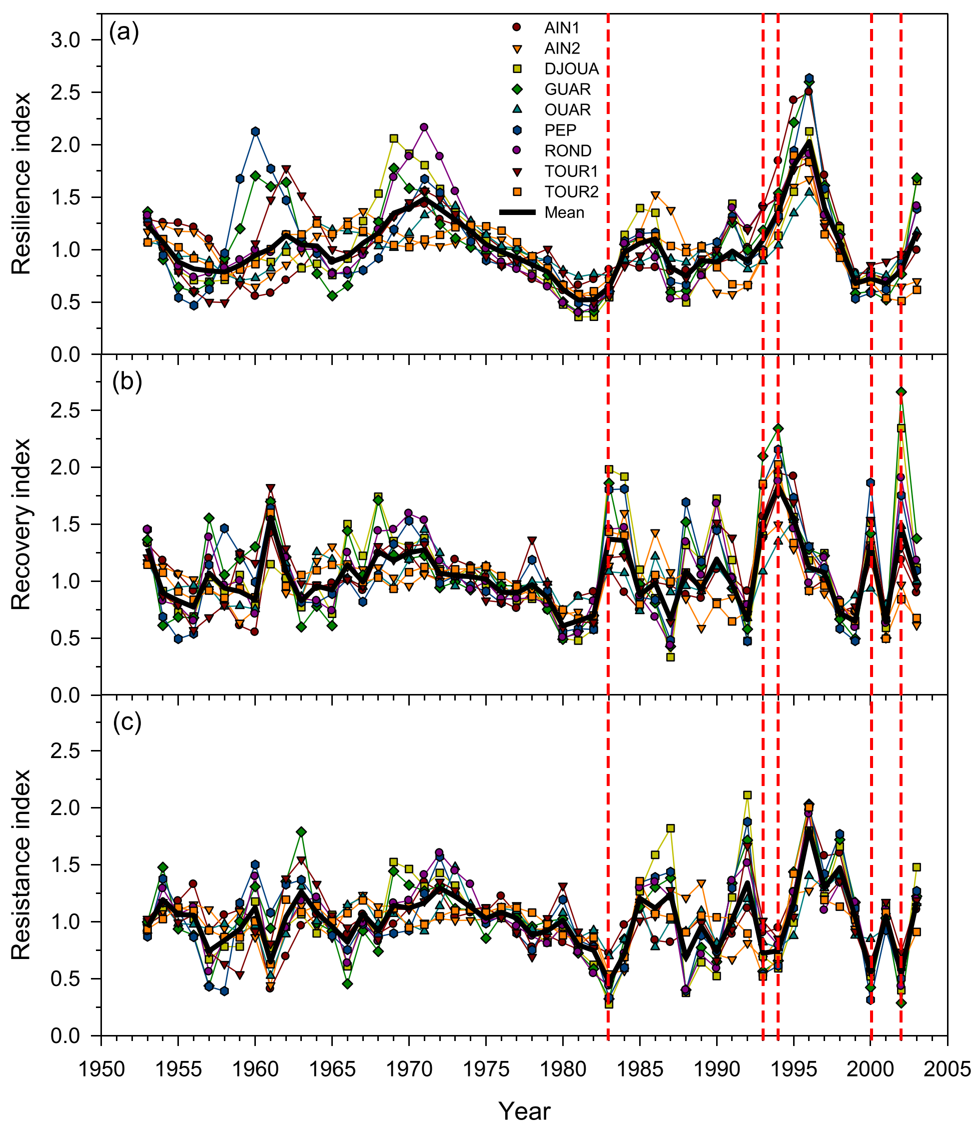

Fig. 3. Site and mean regional series (thick line) of growth resilience indices: (a) resilience index, (b) recovery index, and (c) resistance index. The vertical dashed lines indicate the considered dry years (1983, 1993, 1994, 2000 and 2002).

than as early-warning signals of impending dieback and tree death. Interestingly, the positive relationship between ring-width autocorrelation and tree diameter suggests that small trees are more sensitive to climate, but this hypothesis needs additional research at the individual level to be tested.

There was variability in resilience among plots as showed by the lowest year-to-year variability in growth (MS) and tree-to-tree synchrony (EPS) found in plots on limestone bedrock (AIN1, AIN2). Those plots also showed the highest resistance levels during dry years indicating they are less negatively impacted by drought. Atlas cedar

Table 4
Trends and temporal variability (CV trend) of the resilience, recovery, and resistance indices calculated for the period 1950–2006. Trends were assessed using the Kendall τ statistic. Variability was calculated as the trend of the coefficient of variation for 20-year long intervals. Significance levels: * $p < 0.05$, * * $p < 0.01$, * ** $p < 0.001$.

Site	Trend			CV trend		
	Resilience	Recovery	Resistance	Resilience	Recovery	Resistance
AIN1	-0.01	-0.04	-0.02	0.50 ***	0.16	0.10
AIN2	-0.17	-0.15	-0.03	0.81 ***	0.71 ***	0.81 ***
TOUR1	0.01	0.04	-0.01	0.21	0.56 ***	0.55 ***
TOUR2	-0.18	-0.14	-0.08	0.81 ***	0.82 ***	0.78 ***
OUAR	-0.06	-0.02	-0.08	0.35 **	0.11	0.27 *
PEP	-0.03	0.07	-0.01	0.20	0.73 ***	0.69 ***
ROND	0.02	0.04	-0.01	0.14	0.71 ***	0.71 ***
DJOUA	0.06	0.09	0.01	0.22	0.70 ***	0.79 ***
GUAR	-0.02	0.02	-0.01	0.37 **	0.76 ***	0.63 ***
Mean	-0.02	0.03	-0.01	0.62 ***	0.77 ***	0.81 ***

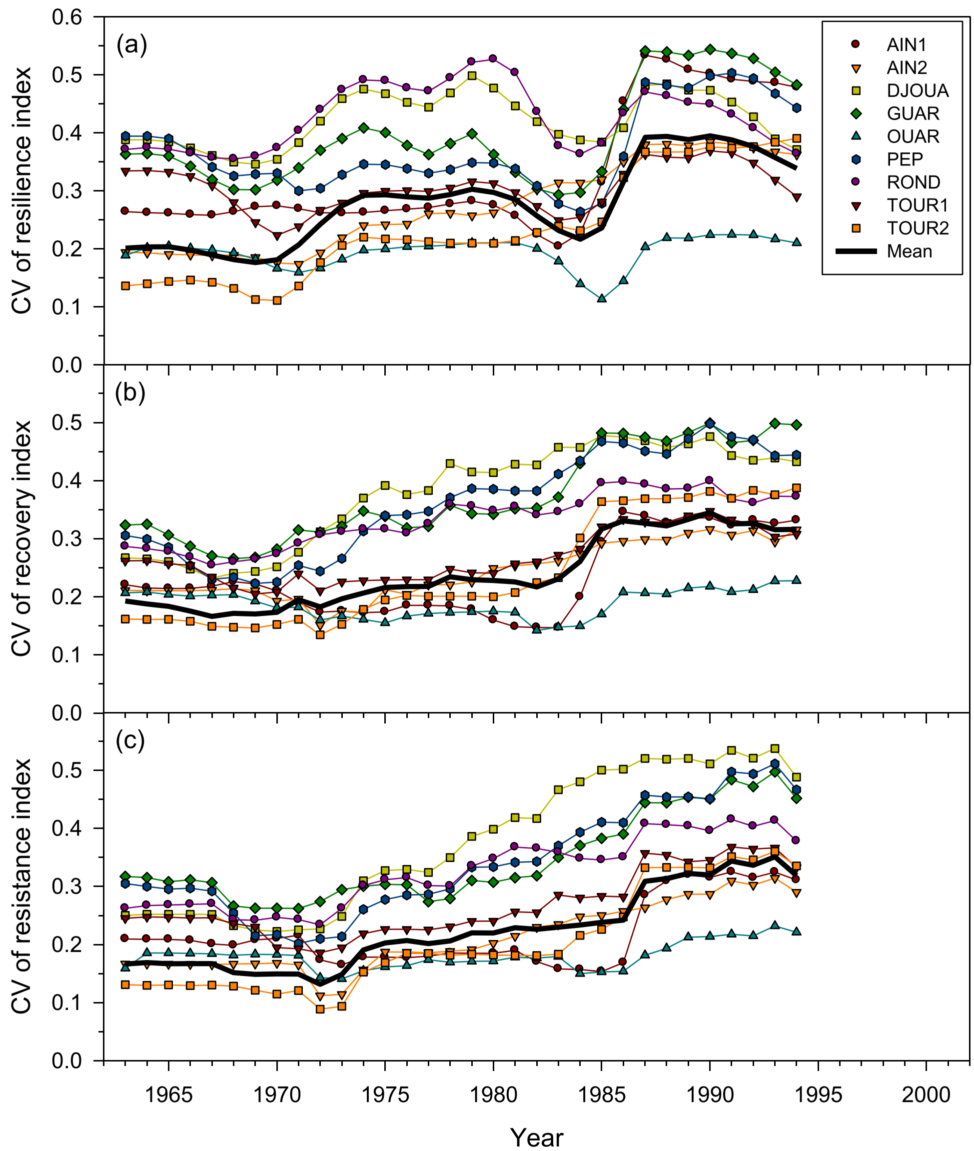

Fig. 4. Site and mean regional series (thick line) of temporal variability of growth (a) resilience, (b) recovery and (c) resistance indices. Variability was calculated as the coefficient of variation (CV) of 20-year moving intervals.

tolerates summer drought but it is vulnerable to long-term, severe droughts and probably cannot update water from deep sources during these lasting dry periods (Aussenac and Finkelstein, 1983; Ladjal et al., 2005, 2007). In the study region, the vulnerability to drought also increased as stand density did and at low elevations where evapotranspiration rates are higher (Sarmoum et al., 2019). However, growth synchrony among trees (EPS) increased as site elevation did whereas the resilience index decreased. This suggests a high responsiveness to water

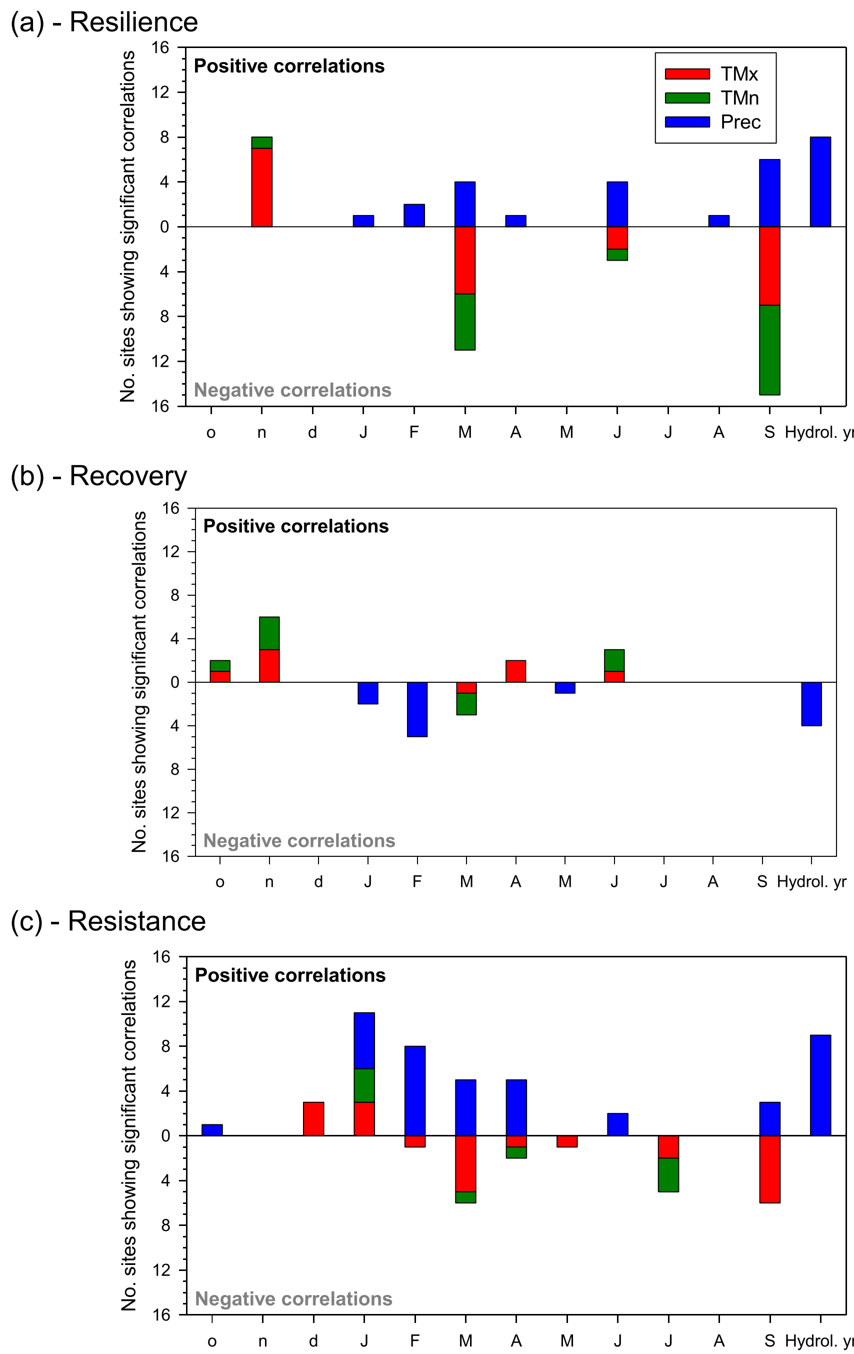

Fig. 5. Number of sites showing significant ($p < 0.05$) positive and negative Pearson correlations between monthly climate variables and site series of (a) resilience, (b) recovery and (c) resistance indices. Climate variables include mean maximum (TMx) and minimum (TMn) temperatures and total precipitation (Prec), which were calculated at monthly and annual (hydrological year) scales. Correlations were calculated from October of the prior year (months abbreviated by lowercase letters) to September of the current year (months abbreviated by uppercase letters).

shortage and a low ability to recover after drought in some high-elevation stands, which are prone to dieback and massive mortality as observed in other Algerian regions (Kherchouche et al., 2012, 2013). The decrease of growth resilience with elevation during dry years was unexpected since conditions are cooler and moister upwards. This pattern may be explained by non-climatic factors leading to water shortage in high-elevation sites such as higher tree-to-tree competition for soil water, steeper slopes or shallow and rocky and poor soils with deep and less accessible groundwater sources (Heydari et al., 2023).

Overall, site environmental factors play relevant roles in modulating how Atlas cedar growth, resilience and vitality respond to drought. Nevertheless, further research should also consider extending these analyses at the individual level to determine if functional traits (e.g., height, wood density, specific leaf area) or genetic differences among stands, which can be legacies of glacial refugia and post-glacial migration (Cheddadi et al., 2017), contribute to acclimation or predispose cedars to growth decline after drought. For instance, growth and isotope data could be combined to assess vulnerability, water- and nutrient-use efficiency in stands or trees with different vigor on limestone and sandstone bedrocks. In addition, resilience metrics should be updated and improved given the limitations detected in widely used tree growth indices (Schwarz et al., 2020).

The presented results echo other findings obtained in other regions of the world. For instance, in the northern Patagonia (Argentina),

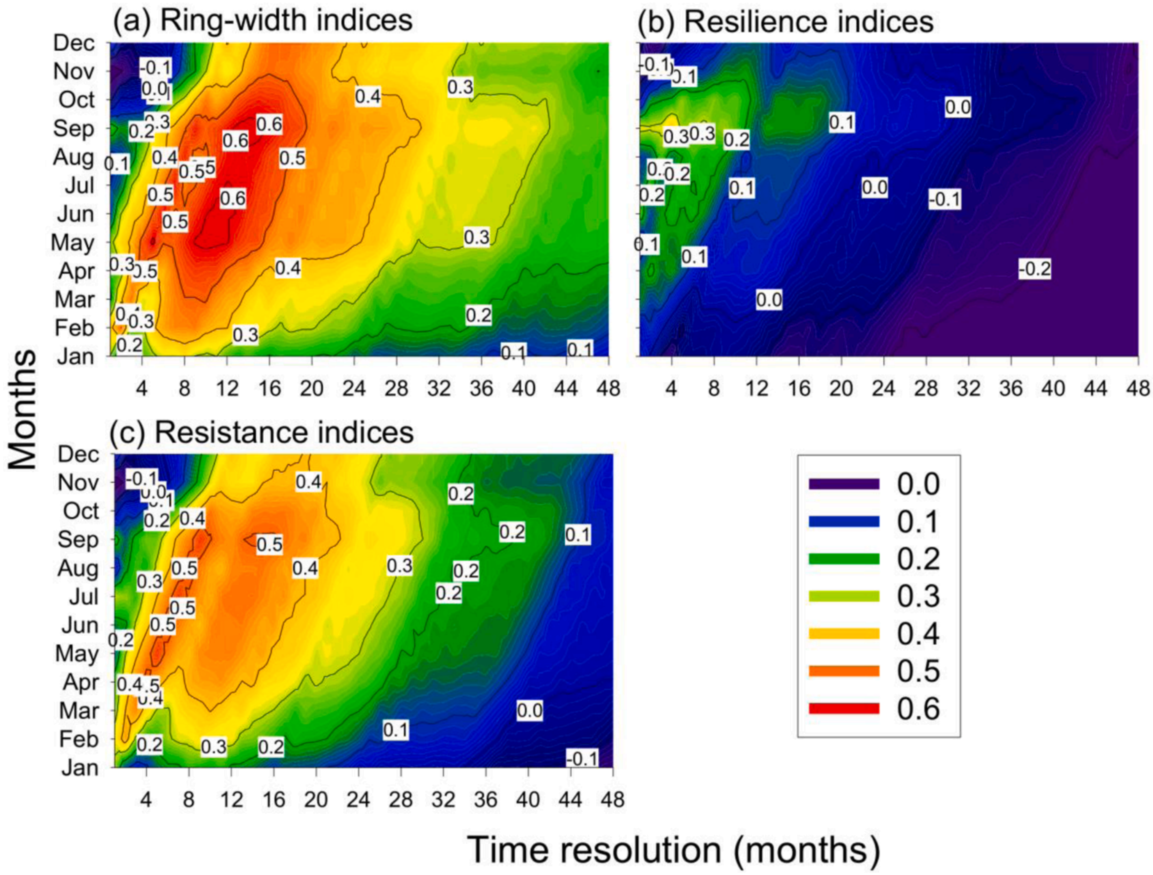

Fig. 6. Correlations calculated by relating monthly values of the SPEI drought index with 1–48 resolution (x axes) and the regional series of: (a) ring-width indices, (b) resilience index and (c) resistance index. The color scales indicate the values of Pearson correlation coefficients.

Austrocedrus chilensis trees showing high resistance during droughts were located in wetter sites (Marcotti et al., 2021). Gazol et al., (2017, 2018, 2020) also found higher resistance levels in wet sites at global and country (Spain) scales. Declining resilience was linked to higher tree mortality in xeric mountain forests from western USA (Cabon et al., 2023). In gymnosperms, drought-related mortality risk is higher in trees with lower resistance, which may be related with lower carbon reserves or tighter stomatal regulation (DeSoto et al., 2020). However, the spatial and temporal dimensions of resistance may differ since we did not observe a long-term decline in resistance as has been reported for gymnosperms at a global scale (Li et al., 2020). Alternatively, resistance showed a higher temporal variability as climate shifted towards drier conditions in the 1980s.

Resistance is just an aspect of tree growth but intra-annual plasticity should be also considered when analyzing the impacts of droughts on forests (Camarero et al., 2018; Zlobin, 2022). In the case of North African Atlas cedar forests, the increase in anthropogenic pressures during the 20th century (cutting, overgrazing, wildfires, tourism…etc.) may have also predisposed to recent drought-triggered damage through soil degradation in some places (Sarmoum et al., 2018; Camarero et al., 2020). Thus, adaptive silviculture techniques enhancing resistance and resilience of Atlas cedar forests should consider reducing competition for water, particularly in winter, and improving the access to soil water and nutrient pools.

5. Conclusions

Atlas cedar growth is tightly coupled with winter precipitation and constrained by long and severe droughts, linked to positive NAO phases, which trigger growth decline and tree death. Analogously, growth resistance is reduced by dry conditions from winter to spring. The resistance-drought relationship has strengthened after the shift towards drier conditions in the 1980s. Cedar stands showing high resistance levels are good candidates as seed sources for future planting programs. Stands showing severe drought damage and a loss in growth resilience should be managed to alleviate water shortage through mitigation measures such as thinning.

Atlas cedar stands inhabiting xeric-warm sites on sandstones and showing low resistance indices may show stronger impacts of drought and be prone to show dieback and high mortality rates if more arid conditions occur, specifically low precipitation in winter accompanied by elevated atmospheric demand (high vapor pressure deficit) in spring and summer. Future cedar grove management plans and planting programs must take these results into consideration by reducing competition for soil water or planting in sites where atmospheric water demand is lower or may be buffered by other tree species or by favorable topoclimatic conditions. Our study was limited by focusing on site or population mean growth responses. Therefore, further research should consider analyzing the intra-specific variability in Atlas cedar growth resilience to drought by quantifying functional traits related to the leaf and wood ecological spectra. This would help selecting those traits or individuals showing higher tolerance to air and soil drought.

CRediT authorship contribution statement

Camarero J. Julio: Writing – review & editing, Writing – original draft, Visualization, Supervision, Software, Methodology, Investigation, Formal analysis, Data curation, Conceptualization. **Sarmoum Mohamed:** Writing – review & editing, Visualization, Validation, Supervision, Software, Resources, Project administration, Methodology,

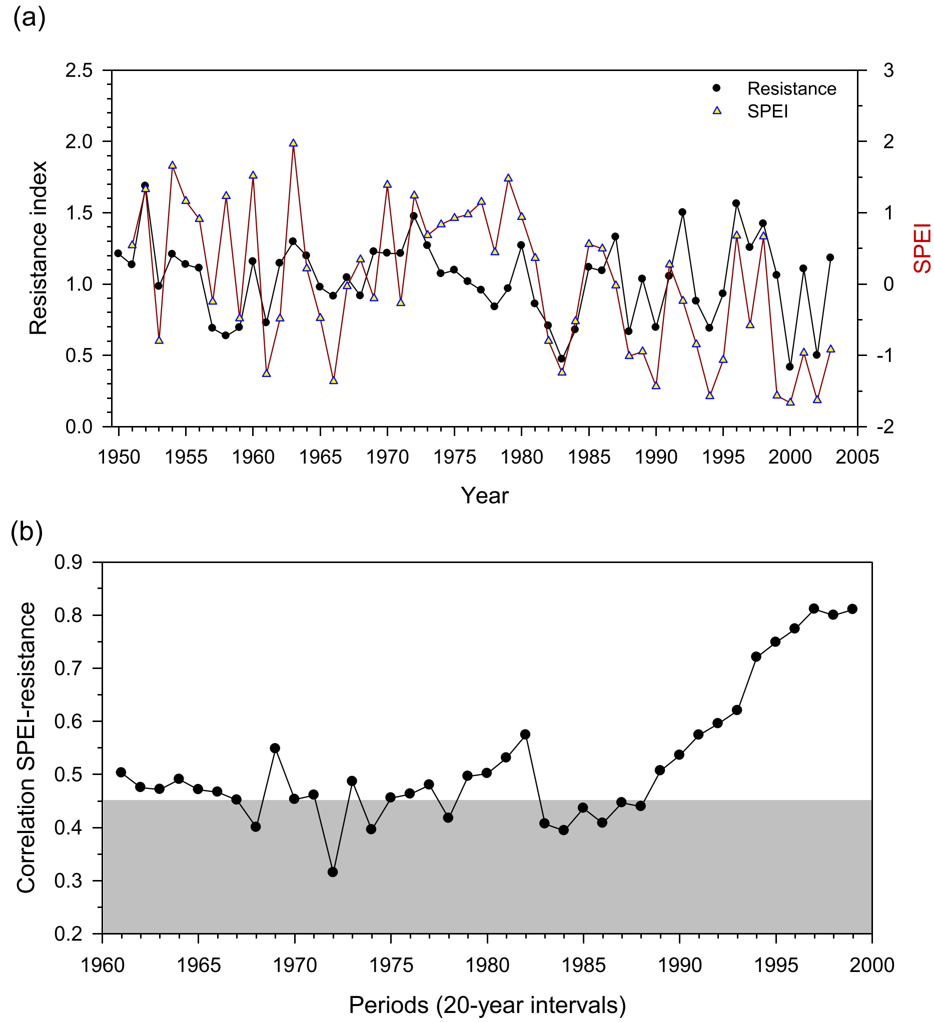

Fig. 7. (a) Regional series of the resistance index and the 8-month August SPEI drought index. (b) Moving correlations between both series considering 20-year moving intervals. Correlation coefficients higher than $r = 0.45$ (gray box in the lower plot) are significant ($p < 0.05$).

Investigation, Funding acquisition, Formal analysis, Data curation, Conceptualization. **Abdoun Fatiha:** Writing – review & editing, Visualization, Validation, Supervision, Resources, Methodology, Investigation, Data curation, Conceptualization.

Declaration of Competing Interest

Authors declare no conflict of interest.

Data availability

Data will be made available on request.

Acknowledgments

This work was funded through PRFU (D00L02UN140120230003) and benefited the support of the general directorate of scientific research and technological development (DGRSDT, MESRS, Algeria) and the University of Tiaret (Algeria) through the financing of mobility internships (IPE-CSIC, Spain). JJC acknowledges funding by the Spanish Ministry of Science and Innovation (projects PID2021–123675OB-C43 and TED2021–129770B-C21). The authors thank the Algerian Ministry of Agriculture and Directorate General of Forests for their permission to work in the "Theniet El Had" National Park. We thank Abdelkader Masloub ("Theniet El Had" National Park, Algeria) for his valuable assistance during fieldwork.

Appendix A. Supporting information

Supplementary data associated with this article can be found in the online version at doi:10.1016/j.foreco.2024.121730.

References

Allen, C.D., Breshears, D.D., McDowell, N.G., 2015. On underestimation of global vulnerability to tree mortality and forest die-off from hotter drought in the Anthropocene. Ecosphere 6, 1–55.
Anderegg, W.R.L., Schwalm, C., Biondi, F., Camarero, J.J., Koch, G., et al., 2015. Pervasive drought legacies in forest ecosystems and their implications for carbon cycle models. Science 349, 528–532.
Aussenac, G., Finkelstein, D., 1983. Influence de la sécheresse sur la croissance et la photosynthèse du cèdre. Ann. Sci. 40, 67–77.
Barcikowska, M.J., Kapnick, S.B., Feser, F., 2018. Impact of large-scale circulation changes in the North Atlantic sector on the current and future Mediterranean winter hydroclimate. Clim. Dyn. 50, 2039–2059. https://doi.org/10.1007/s00382-017-3735-5.
Bentouati, A., 2008. La situation du cèdre de l'Atlas dans les Aurès (Algérie). For. Méditerranéenne 29, 203–208.
Briffa, K.R., Jones, P.D., 1990. Basic chronology statistics and assessment. In: Cook, E.R., Kairiukstis, L.A. (Eds.), Methods of Dendrochronology, Kluwer, Dordrecht, pp. 137–152.
Bunn, A.G., 2008. A dendrochronology program library in R (dplR). Dendrochronologia 26, 115–124. https://doi.org/10.1016/j.dendro.2008.01.002.
Bunn, A.G., 2010. Statistical and visual crossdating in R using the dplR library. Dendrochronologia 28, 251–258. https://doi.org/10.1016/j.dendro.2009.12.001.

Bunn, A.G., Korpela, M., Biondi, F., Campelo, F., Mérian, P., Qeadan, F., Zang, C., 2023. dplR: Dendrochronology Program Library in R. R package version 1.7.5, ⟨https://CRAN.R-project.org/package=dplR⟩.
Cabon, A., DeRose, R.J., Shaw, J.D., Anderegg, W.R.L., 2023. Declining tree growth resilience mediates subsequent forest mortality in the US Mountain West. Glob. Ch. Biol. 29, 4826–4841.
Cailleret, M., Dakos, V., Jansen, S., Robert, E.M., Aakala, T., Amoroso, M.M., Antos, J.A., Bigler, C., Bugmann, H., Caccianiga, M., Camarero, J.J., et al., 2019. Early-warning signals of individual tree mortality based on annual radial growth. Front. Plant Sc. 9 https://doi.org/10.3389/fpls.2018.01964.
Camarero, J.J., 2011. Direct and indirect effects of the North Atlantic oscillation on tree growth and forest decline in northeastern Spain. In: Vicente-Serrano, S.M., Trigo, R. M. (Eds.), Hydrological, Socioeconomic and Ecological Impacts of the North Atlantic Oscillation in the Mediterranean Region. Springer, pp. 129–152.
Camarero, J.J., Gazol, A., Sangüesa-Barreda, G., Oliva, J., Vicente-Serrano, S.M., 2015. To die or not to die: early warnings of tree dieback in response to a severe drought. J. Ecol. 103, 44–57.
Camarero, J.J., Gazol, A., Sangüesa-Barreda, G., Cantero, A., Sánchez-Salguero, R., Sánchez-Miranda, A., Granda, E., Serra-Maluquer, X., Ibañez, R., 2018. Forest growth responses to drought at short- and long-term scales in Spain: squeezing the stress memory from tree rings. Front. Ecol. Evol. 6, 9.
Camarero, J.J., Sánchez-Salguero, R., Sangüesa-Barreda, G., Lechuga, V., Viñegla, B., Seco, J.I., Taïqui, L., Carreira, J.A., Linares, J.C., 2020. Drought, axe and goats. More variable and synchronized growth forecasts worsening dieback in Moroccan Atlas cedar forests. Sci. Tot. Env. 15, 142752.
Camarero, J.J., Gazol, A., Colangelo, M., Linares, J.C., Navarro-Cerrillo, R.M., Rubio-Cuadrado, A., Silla, F., Dumas, P.-J., Courbet, F., 2022. Shifting precipitation patterns drive growth variability and drought resilience of European Atlas cedar plantations. Forests 12, 1751.
Cheddadi, R., Henrot, A., François, L., Boyer, F., Bush, M., Carré, M., et al., 2017. Microrefugia, climate change, and conservation of *Cedrus atlantica* in the Rif mountains, Morocco. Front. Ecol. Evol. 5, 114.
Cook, E.R., Seager, R., Kushnir, Y., Briffa, K.R., Buntgen, U., Frank, D., et al., 2015. Old World megadroughts and pluvials during the Common Era. Sci. Adv. 1 https://doi.org/10.1126/sciadv.1500561.
Dakos, V., Scheffer, M., van Nes, E.H., Brovkin, V., Petoukhov, V., Held, H., 2008. Slowing down as an early warning signal for abrupt climate change. PNAS 105, 14308–14312.
Dakos, V., Carpenter, S.R., van Nes, E.H., Scheffer, M., 2015. Resilience indicators: prospects and limitations for early warnings of regime shifts. Philos. Trans. R. Soc. Ser. B 370, 20130263. https://doi.org/10.1098/rstb.2013.0263.
DeSoto, L., Cailleret, M., Sterck, F., Jansen, S., Kramer, K., et al., 2020. Low growth resilience to drought is related to future mortality risk in trees. Nat. Comm. 11, 545 https://doi.org/10.1038/s41467-020-14300-5.
Esper, J., Frank, D., Verstege, A., Luterbacher, J., Xoplaki, E., 2007. Long-term drought severity variations in Morocco. Geophys. Res. Lett. 34. L17702.
Fritts, H.C., 1976. Tree Rings and Climate. Academic Press, London.
Gaussen, H., 1956. Le XVIII congres international de Geographie, Rio de Janeiro, Aout 1956. Ann. De. Geogr. (353), 1–19.
Gazol, A., Camarero, J.J., Anderegg, W.R.L., Vicente-Serrano, S.M., 2017. Impacts of droughts on the growth resilience of northern hemisphere forests. Glob. Ecol. Biogeogr. 26, 166–176.
Gazol, A., Camarero, J.J., Vicente-Serrano, S.M., et al., 2018. Forest resilience to drought varies across biomes. Glob. Change Biol. 24, 2143–2158.
Gazol, A., Camarero, J.J., Sánchez-Salguero, R., Vicente-Serrano, S.M., et al., 2020. Drought legacies are short, prevail in dry conifer forests and depend on growth variability. J. Ecol. 108, 2473–2484.
Giorgi, F., Lionello, P., 2008. Climate change projections for the Mediterranean region. Glob. Planet Chang 63, 90–104.
Harris, I., Osborn, T.J., Jones, P., Lister, D., 2020. Version 4 of the CRU TS monthly high-resolution gridded multivariate climate dataset. Sci. Data 7, 109. https://doi.org/10.1038/s41597-020-0453-3.
Heydari, M., Cheraghi, J., Omidipour, R., Rostaminia, M., Kooch, Y., Valko, O., Carcaillet, C., 2023. Tree dieback, woody plant diversity, and ecosystem driven by topography in semi-arid mountain forests: implication for ecosystem management. J. Env. Manag. 339, 117892.
Holmes, R.L., 1983. Computer-assisted quality control in tree-ring dating and measurement. Tree-Ring Bull. 43, 69–78.
Hurrell, J., 1995. Decadal trends in North Atlantic Oscillation and relationship to regional temperature and precipitation. Science 269, 676–679.
Hurrell, J., Van Loon, H., 1997. Decadal variations in climate associated with the North Atlantic Oscillation. Clim. Change 36, 301–326.
Hurrell, J., Kushnir, Y., Ottersen, G., Visbeck, M., 2003. An overview of the North Atlantic Oscillation. The North Atlantic Oscillation: climate significance and environmental impact. Geophys Monogr. 134, 1–36.
Jones, P.D., Jónsson, T., Wheeler, D., 1997. Extension to the North Atlantic Oscillation using early instrumental pressure observations from Gibraltar and South-West Iceland. Int. J. Climatol. 17, 1433–1450.
Kherchouche, D., Kalla, M., Gutiérrez, E., Attalah, S., Bouzghaia, M., 2012. Impact of droughts on *Cedrus atlantica* forests dieback in the Aurès. (Algeria). J. Life Sci. 6, 1262–1269.
Kherchouche, D., Kalla, M., Gutiérrez, E., Briki, A., Hamchi, A., 2013. La sécheresse et le dépérissement du cèdre de l'Atlas (Cedrus atlantica Manetti) dans le massif du Belezma (Algérie). Sci. Et. Chang. planétaires/Sécheresse 24, 129–137.
Ladjal, M., Huc, R., Ducrey, M., 2005. Drought effects on hydraulic conductivity and xylem vulnerability to embolism in diverse species and provenances of Mediterranean cedars. Tree Physiol. 25, 1109–1117.
Ladjal, M., Deloche, N., Huc, R., Ducrey, M., 2007. Effects of soil and air drought on growth, plant water status and leaf gas exchange in three Mediterranean cedar species: *Cedrus atlantica*, *C. brevifolia* and *C. libani*. Trees Struct. Funct. 21, 201–213.
Li, X., Piao, S., Wang, K., Wang, X., Wang, T., Ciais, P., Chen, A., Lian, X., Peng, S., Peñuelas, P., 2020. Temporal trade-off between gymnosperm resistance and resilience increases forest sensitivity to extreme drought. Nat. Ecol. Evol. 4, 1075–1083. https://doi.org/10.1038/s41559-020-1217-3.
Linares, J.C., Taiqui, L., Camarero, J.J., 2011. Increasing drought sensitivity and decline of atlas Cedar (*Cedrus atlantica*) in the Moroccan Middle Atlas Forests. Forests 2, 777–796. https://doi.org/10.3390/f2030777.
Linares, J.C., Taïqui, L., Sangüesa-Barreda, G., Seco, J., Camarero, J.J., 2013. Age-related drought sensitivity of Atlas cedar (*Cedrus atlantica*) in the Moroccan Middle Atlas forests. Dendrochronologia 31, 88–96.
Lloret, F., Keeling, E.G., Sala, A., 2011. Components of tree resilience: effects of successive low-growth episodes in old ponderosa pine forests. Oikos 120, 1909–1920.
Marcotti, E., Amoroso, M.M., Rodríguez-Catón, M., Vega, L., Srur, A.M., Villalba, R., 2021. Growth resilience of *Austrocedrus chilensis* to drought along a precipitation gradient in Patagonia, Argentina. For. Ecol. Manag. 496, 119388 https://doi.org/10.1016/j.foreco.2021.119388.
Messaoudene, M., Rabhi, K., Megdoud, A., Sarmoum, M., Dahmani-Megrerouche, M., 2013. Etat des lieux et perspectives des cédraies algériennes. For. Méditerranéenne 4, 1–8.
Navarro-Cerrillo, R.M., Manzanedo, R.D., Bohorque, J., Sánchez-Salguero, R., Sánchez, J., de Miguel, S., Solano, D., Qarro, M., Griffith, D., Palacios, G., 2013. Structure and spatio-temporal dynamics of cedar forests along a management gradient in the Middle Atlas, Morocco. . Ecol. Manag. 289, 341–353. https://doi.org/10.1016/j.foreco.2012.10.011.
Navarro-Cerrillo, R.M., Sarmoum, M., Gazol, A., Abdoun, F., Camarero, J.J., 2019. The decline of Algerian *Cedrus atlantica* forests is driven by a climate shift towards drier conditions. Dendrochronologia 55, 60–70. https://doi.org/10.1016/j.dendro.2019.04.003.
Oksanen, J., Simpson, G., Blanchet, F., Kindt, R., Legendre, P. et al., 2023. vegan: Community Ecology Package. R package version 2.6–5, ⟨https://github.com/vegandevs/vegan⟩.
Padrón, R.S., Gudmundsson, L., Decharme, B., et al., 2020. Observed changes in dry-season water availability attributed to human-induced climate change. Nat. Geosci. 13, 477–481. https://doi.org/10.1038/s41561-020-0594-1.
R Core Team. 2023. R: A language and environment for statistical computing. Vienna, Austria: R Foundation for Statistical Computing. ⟨https://www.R-project.org/⟩.
Reynolds, R.W., Smith, T.M., Liu, C., Chelton, D.B., Casey, K., Schlax, M.G., 2007. Daily high-resolution-blended analyses for sea surface temperature. J. Clim. 20, 5473–5496.
Sarmoum, M., Navarro-Cerrillo, R.M., Guibal, F., Abdoun, F., 2018. Structure, tree growth, dynamics and management of *Cedrus atlantica* Manetti forests in Theniet El Had National Park (N-W Algeria). Open J. Ecol. 8, 432–446.
Sarmoum, M., Navarro-Cerrillo, R.M., Guibal, F., Abdoun, F., 2019. Impact of drought and site characteristics on vitality and radial growth of *Cedrus atlantica* Manetti in the Ouarsenis massif (Algeria). AGROFOR 4, 42–52. https://doi.org/10.7251/AGRENG1903042S.
Satoh, Y., Yoshimura, K., Pokhrel, Y., et al., 2022. The timing of unprecedented hydrological drought under climate change. Nat. Comm. 13, 3287 https://doi.org/10.1038/s41467-022-30729-2.
Scheffer, M., Bascompte, J., Brock, W., Brovkin, V., Carpenter, S.R., Dakos, V., Held, H., van Nes, E.H., Rietkerk, M., Sugihara, G., 2009. Early-warning signals for critical transitions. Nature 461, 53–59.
Schwarz, J., Skiadaresis, G., Kohler, M., Kunz, J., Schnabel, F., Vitali, V., Bauhus, J., 2020. Quantifying growth responses of trees to drought—a critique of commonly used resilience indices and recommendations for future studies. Curr. . Rep. 6, 185–200.
Slimani, S., Derridj, A., Gutiérrez, E., 2014. Ecological response of *Cedrus atlantica* to climate variability in the Massif of Guetiane (Algeria). For. Syst. 23, 448–460.
Speer, J., 2010. Fundamentals of Tree-Ring Research. The University of Arizona Press, Tucson, Arizona.
Stokes, M.A., Smiley, T.L., 1968. An Introduction to Tree-Ring Dating. University of Chicago Press, Chicago, USA.
Touchan, R., Anchukaitis, K., Meko, D., Sabir, M., Attalah, S., Aloui, A., 2011. Spatiotemporal drought variability in Northwestern Africa over the last nine centuries. Clim. Dyn. 37, 237–252.
van der Maaten-Theunissen, M., van der Maaten, E., Bouriaud, O., 2015. pointRes: an R package to analyze pointer years and components of resilience. Dendrochronologia 35, 34–38. https://doi.org/10.1016/j.dendro.2015.05.006.
van der Maaten-Theunissen, M., Trouillier, M., Schwarz, J., Skiadaresis, G., Thurm, E.A., van der Maaten, E., 2021. pointRes 2.0: new functions to describe tree resilience. Dendrochronologia 70, 125899. https://doi.org/10.1016/j.dendro.2021.125899.
Wang, B., Chen, T., Xu, G., Wu, G., Liu, G., 2023. Management can mitigate drought legacy effects on the growth of a moisture-sensitive conifer tree species. For. Ecol. Manag. 544, 121196 https://doi.org/10.1016/j.foreco.2023.121196.

Wigley, T.M.L., Briffa, K.R., Jones, P.D., 1984. On the average value of correlated timeseries, with applications in dendroclimatology and hydrometeorology. J. Clim. Appl. Meteorol. 23, 201–213.

Zang, C., Biondi, F., 2015. treeclim: an R package for the numerical calibration of proxy-climate relationships. Ecography 38, 431–436. https://doi.org/10.1111/ecog.01335.

Zlobin, I.E., 2022. Linking the growth patterns of coniferous species with their performance under climate aridization. Sci. Tot. Env. 831, 154971.